IOPscience iopscience.iop.org

Home Search Collections Journals About Contact us My IOPscience

Molecular Dynamics Analysis of Effects of Velocity and Loading on the Nanoindentation

This content has been downloaded from IOPscience. Please scroll down to see the full text.

2002 Jpn. J. Appl. Phys. 41 L1328

(http://iopscience.iop.org/1347-4065/41/11B/L1328)

View the table of contents for this issue, or go to the journal homepage for more

Download details:

IP Address: 140.113.38.11
This content was downloaded on 28/04/2014 at 03:57

Please note that terms and conditions apply.

Jpn. J. Appl. Phys. Vol. 41 (2002) pp. L 1328–L 1331
Part 2, No. 11B, 15 November 2002
©2002 The Japan Society of Applied Physics

Molecular Dynamics Analysis of Effects of Velocity and Loading on the Nanoindentation

Te-Hua FANG*, Sheng-Rui JIAN[1] and Der-San CHUU[1]

Department of Mechanical Engineering, Southern Taiwan University of Technology, Tainan 710, Taiwan, R.O.C.
[1]*Institute and Department of Electrophysics, National Chiao Tung University, Hsinchu 300, Taiwan, R.O.C.*

(Received September 26, 2002; accepted for publication October 21, 2002)

Three-dimensional molecular dynamics (MD) simulation is used to investigate the atomistic mechanism of nanoindentation process under various indentation loads and velocities that occur when a diamond tip interacts with the copper thin film. In this study, the model utilizes the Morse potential function to simulate interatomic forces between the specimen and tip. The results show that both Young's modulus and hardness increase up to a critical value and decrease there after for the indentation velocities, but decrease as the indentation loads increase. In additional, the contact stress-strain relationship is shown to be important. [DOI: 10.1143/JJAP.41.L1328]

KEYWORDS: molecular dynamics, nanoindentation, Young's modulus, hardness, contact stress strain

Due to the improvements in manufacturing technology, the thickness of films in semiconductors or MEMS devices has broken the sub-micrometer barrier and now has reached the nanometer level. However, there is a marked difference between the physical characteristics of films with thickness on the micrometer scale, and those with thickness on the nanometer scale. In order to clearly understand these differences, it is essential to investigate the physical properties of thin films. Nanoindentation is the most frequently used technique for measuring thin film properties such as Young's modulus and hardness. Research in this area is partially summarized in reference.[1] However, in order to obtain precise measure film properties, especially for very thin films of the order of less than 1-nm thick, significant redesign and improvement of nanoindentation measurement systems, with special emphasis on tips, is required.[2,3] Current systems have difficulty maintaining controlled and reliable small depth penetration, which is required for minimizing substrate influences during thin film measurements.

Various aspects of the interaction between tool tip and specimen during the nanoindentation process have been investigated. This in previous studies has included the phenomena of tip-specimen adhesion and specimen fracture of the specimen,[4,5] nanoscale etching and indentation using carbon nanotube,[6] phase transformations,[7,8] elastic and plastic contact behavior,[9] and the influence of different tool materials on the indentation mechanism.[10] These previous studies provide significant insight into tip-specimen interaction phenomena.[11] However, the effect of indentation velocities and contact stress and strain are also important in the nanoindentation process. Thus based on these viewpoints, the main object of this study is to evaluate these effects on the nanoindentation processes by using the molecular dynamics (MD) simulation.

In most previous studies the MD simulation method has been used to investigate phenomena occurring during the nanoindentation process. It is proposed to use the same method for this study. MD simulation of nanoindentation is used to investigate various aspects of the interaction between a rigid diamond tip and a monocrystalline copper film. Periodic boundary conditions[12] are used in the transverse (x- and y-directions), and the bottom three layers of atoms of the copper are fixed in space.[13] The force acting on an individual atom is obtained by summing the forces contributed by the surrounding atoms. The Morse potential is written as

$$\phi(r_{ij}) = D\{\mathrm{e}^{-2\alpha(r_{ij}-r_0)} - 2\mathrm{e}^{-\alpha(r_{ij}-r_0)}\} \quad (1)$$

where $\phi(r_{ij})$ is a pair potential energy function, D, α, and r_0 correspond to the cohesion energy, the elastic modulus and the atomic distance at equilibrium, respectively. Their related parameters are shown in Table I.[14] The Morse potential has been selected for these simulations because it is simple and computationally inexpensive, and it has been used previously in several similar studies.[15]

The force on atom i resulting from the interaction of all the other atoms can be derived from the above potential function, eq. (1) such that

$$F_i = -\sum_{\substack{j=1 \\ (j\neq i)}}^{N} \nabla_i \phi(r_{ij}) = m_i \frac{d^2 r_i(t)}{dt^2} \quad (2)$$

where F_i is the resultant force on atom i, m_i is the mass of atom i, r_i is the position of atom i, and N is the total number of atoms. The data (tip velocity, integration time, etc.) are input, the initial configuration of the sample material is a face-centered cubic (FCC) copper lattice. Initial velocities are assigned from the Maxwell distribution, and the magnitudes are adjusted so as to keep the temperature in the system constant according to

$$V_i^{\mathrm{new}} = \left\{ \frac{N_\mathrm{f} N k_\mathrm{B} T_0}{2} \left[\sum_{i=1}^{N} \frac{m_i (V_i^{\mathrm{old}})^2}{2} \right]^{-1} \right\}^{\frac{1}{2}} \cdot V_i^{\mathrm{old}} \quad (3)$$

where V_i is the velocity of atom i, T_0 is a specified temperature, k_B is Boltzmann's constant ($= 1.381 \times 10^{-23}\ \mathrm{JK}^{-1}$), and N_f is the freedom of the system. The initial displacement and velocity are values determined independently, and the time integration of motion is performed by Gear's fifth predictor-

Table I. Parameters in the Morse potential.

Parameter	Cu–Cu	Cu–C	C–C
D (eV)	0.3429	0.100	2.423
α (10^{10} m^{-1})	1.3558	1.700	2.555
r_0 (10^{-10} m)	2.6260	0.220	2.522

*Author to whom all the correspondence should be addressed. E-mail address: fang@mail.stut.edu.tw

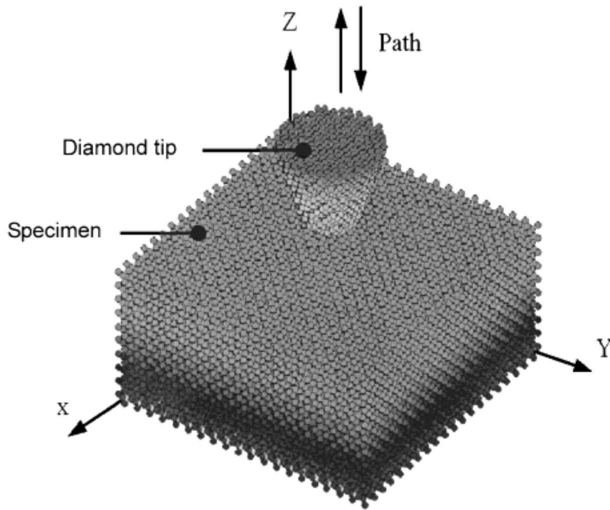

Fig. 1. Molecular dynamic simulation model.

corrector method.[12] The copper thin film and a diamond tip tool are used in these simulations. The direction of indentation vertical to the specimen surface is taken as the negative z-axis, as seen in Fig. 1. In preparation for this study, films with different numbers of atoms per layer and different numbers of layers were tested, with the intention of only selecting films that were thin enough to prevent the film thickness affecting the simulation results. Thus, in this study films with 16,000 atoms (800 atoms/layer, 20 layers) are used. This is not claimed to be a truly minimum array, but is rather an empirically derived practical array. It was found that thickness effects are quite acceptable with a 20-layer film. For the simulation, the specimen is initially assumed to have a well-defined atomic surface and the time step is set to 1 fs. The atomic array model of the surface is constructed for a specific temperature at equilibrium and the velocities of atoms of the specimen at this state are satisfied with a Maxwell velocity distribution. The Morse potential proposed by Maekawa and Itoh[15] was adopted in this work.

Young's modulus is first calculated using the composition response modulus, E_r, which takes into account the combined elastic effects of indention tip and film:

$$E_r = \frac{1}{2}\sqrt{\frac{\pi}{A_c}}\frac{dP}{dh} \tag{4}$$

where $\frac{dP}{dh}$ is the slope of the beginning of the unloading curve, and A_c is the projected contact area at the maximum load. The final Young's modulus of the specimen, E_s, is obtained from the expression

$$\frac{1}{E_r} = \frac{1-\upsilon_s^2}{E_s} + \frac{1-\upsilon_i^2}{E_i} \tag{5}$$

where E_i is the elastic modulus of the indenter, and υ_s and υ_i are the Poisson's ratios of specimen and indenter, respectively. A key point when determining an elastic modulus from an indention experiment is how to ascertain the projected contact area, A_c. Oliver and Pharr[1] developed an improved technique for the measurement of indentation impressions. They used data directly drawn from the indentation curve and correlated the projected contact area to the contact depth, h_c, as

$$A_c = F(h_c) \tag{6}$$

where h_c may be expressed as

$$h_c = h_{max} - 0.72\frac{P_{max}}{S_{max}} \tag{7}$$

where h_{max} is the maximum depth, P_{max} is the maximum load, and S_{max} is the slope of the unloading curve at the maximum load. The material properties used in this study's calculations are $E_i = 1140$ GPa and $\upsilon_i = 0.07$ for an ideally conical diamond indenter with $R = 2$ nm tip radius and 60° included angle, and $\upsilon_s = 0.3$ for the copper thin film.

The hardness of a material is defined as its resistance to local plastic deformation. Thus, the hardness, H, is determined from the maximum indentation load P_{max} divided by the projected contact area i.e.,

$$H = \frac{P_{max}}{A_c}. \tag{8}$$

To better understand the deformation mechanisms of nanometer-scale, the stress-strain relationship are calculated using the radius a of the contact area to determine the stress using the Hertzian equation,[16]

$$a = \left(\frac{3PR}{4E_r}\right)^{1/3}. \tag{9}$$

In order to investigate the affect of loading and velocity on the nanoindentation process, the process was simulated using various loads and indentation velocities. Figures 2(a) and 2(b) show load-displacement curves for copper thin film under different indentation loads and at different velocities, respectively. With the diamond tip draws back, the plastic deformed region undergoes a partial elastic recovery indicating the irreversibility of the plastic behavior during nanoindentation that manifests in the load-displacement curves as a hysteresis form. As the indentation depth of the diamond tip continues to increase, the load curve starts to go up until it reaches a maximum depth. After reaching the maximum depth, the tip begins to unload and return to its original position. The intersection of the tangent to the topmost third of the unloading curve with the x-axis gives the plastic indentation depth, h_p.[1] The area contained by loading-unloading curves represents the plastic energy. The plastic energy increases with increasing indentation loads as shown in Fig. 2(a). In addition, Fig. 2(b) also indicates that for a given indentation depth, the plastic energy increases as indentation velocities increase. The penetration depth of less than 2 nm is in the plastic zone.

The Young's modulus and hardness of the copper thin film under different loads and at different velocities are evaluated from the indentation curves, as shown in Figs. 3(a) and 3(b), respectively. Young's modulus decreases with increasing load, but the hardness slowly decreases in Fig. 3(a). Both Young's modulus and hardness of different indentation loads are approximately 364.03 GPa–675.30 GPa and 88.38 GPa–110.63 GPa, respectively. On the other hand, the effect of indentation velocities on the Young's modulus and hardness is shown in Fig. 3(b). The Young's modulus and hardness of different indentation velocities are approximately 249.69 GPa–466.04 GPa and 53.05 GPa–101.01 GPa, respectively. The energy of the impact of the indenter on film surface is greater

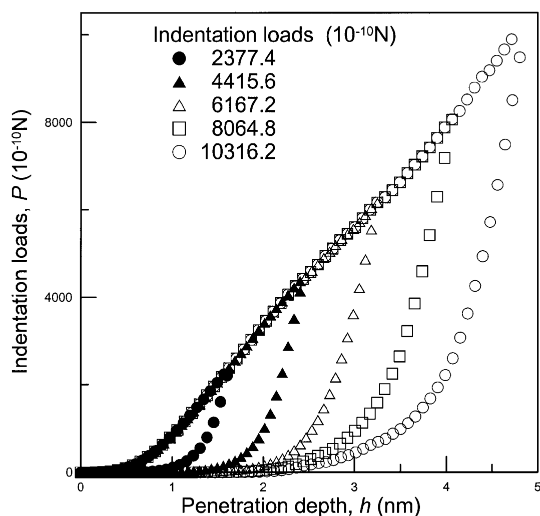

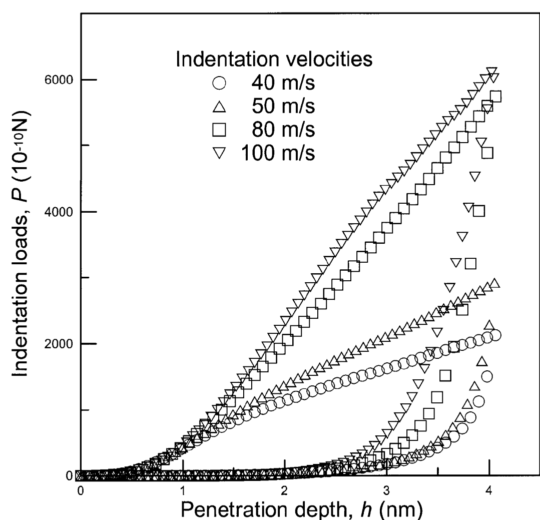

Fig. 2. (a) Load-displacement curves of the different indentation loads, and (b) is shown the curves for the different indentation velocities.

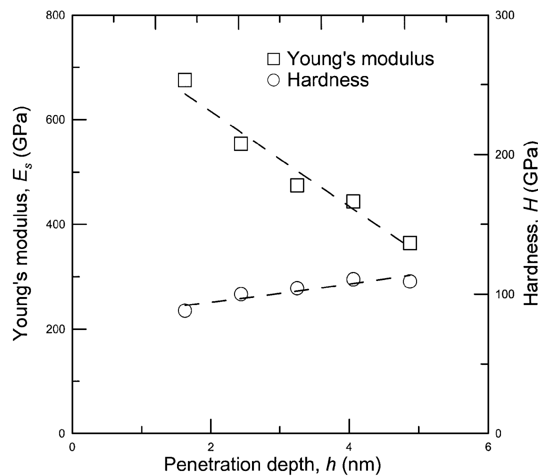

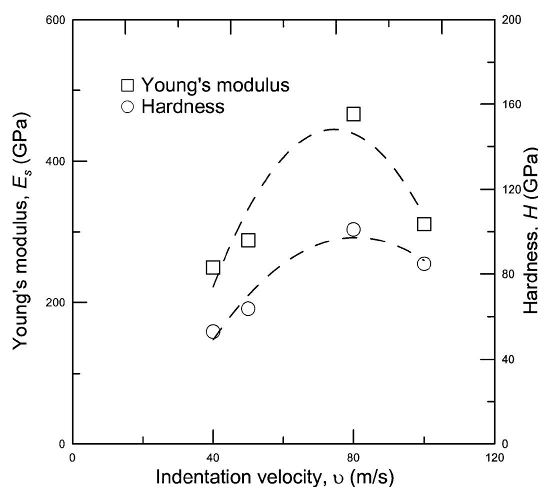

Fig. 3. (a) Young's modulus and Hardness vs. Penetration depth in the different indentation loads, and (b) which is shown in the different indentation velocities.

at the higher velocities, which causes the Young's modulus and hardness to increase up to a critical level. The critical velocity occurs at the indentation velocity of 80 m/s, shown in Fig. 3(b). Above this velocity, the impact causes the copper thin film to yield, and the Young's modulus and hardness are trended to decrease. Therefore, it is important that the indentation velocity can sometimes cause the different surface effects during nanoindentation.

Based on a local strain diagnostic, to identify the plastic behavior during nanoindentation processes. The results of the simulation show, the strain rate increases with increasing loads in Fig. 4(a), which creates an increasing number of dislocations, which in turn causes material deformation. According to the indentation velocities simulation, which is shown in Fig. 4(b), the maximum yielding point of the material is 312.25 GPa at a strain rate of 0.67, the strain rate decreasing there after. This explains why a greater indentation velocity causes a larger kinetic energy to deform the material, but the film can only bear up to a critical value.

In summary, in order to better understand the plastic deformation processes, we have performed the MD simulation of different indentation loads and velocities for copper thin film during nanoindentation. Even for an ultrasmall penetration depth (< 2 nm), the simulation results show copper thin film deform plastically and give a good description. Both Young's modulus and hardness decrease as the indentation loads increase. But, for the indentation velocities simulation part, Young's modulus and hardness decrease at a critical velocity of 80 m/s. In addition, the results also indicate that the indentation velocity which is the main reason to domain the deformation mechanism; the yielding point which occurs at indentation critical velocity 80 m/s is 312.25 GPa. Hence with the aid of MD simulations, the nanoindentation processes of copper thin film and a diamond tip during indentation and the mechanism are clearing shown.

The authors gratefully acknowledge the support to this research by the National Science Council, Republic of China, under Grant Nos. NSC90-2218-E218-011 and NSC91-2218-

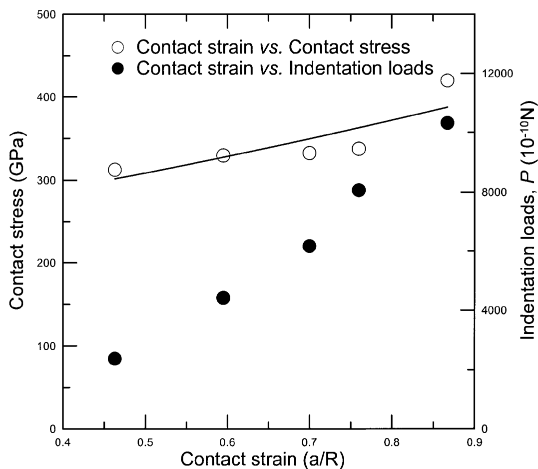

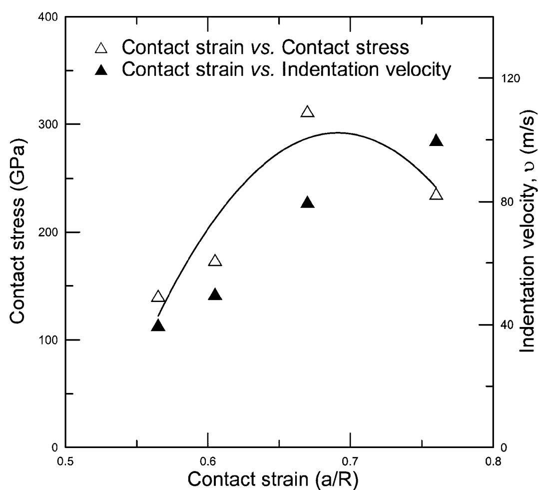

Fig. 4. (a) Schematic diagram showing the contact stress-strain relationship of the different indentation loads, and (b) is shown this relationship for the different indentation velocities.

E218-001.

1) W. C. Oliver and G. M. Pharr: J. Mater. Res. **7** (1992) 1564.
2) B. Bhushan and V. N. Koinkar: Appl. Phys. Lett. **64** (1994) 1653.
3) K. Miyahara, S. Nagashima, T. Ohmura and S. Matsuoka: Nanostruct. Mater. **12** (1999) 1049.
4) U. Landman, W. D. Luedtke, N. A. Burnham and R. J. Colton: Science **248** (1990) 454.
5) J. A. Harrison, C. T. White, R. J. Colton and D. W. Brenner: Surf. Sci. **271** (1992) 57.
6) F. N. Dzegilenko, D. Srivastava and S. Saini: Nanotechnology **10** (1999) 253.
7) W. C. D. Cheong and L. C. Zhang: Nanotechnology **11** (2000) 173.
8) W. C. D. Cheong and L. C. Zhang: J. Mater. Sci. Lett. **19** (2000) 439.
9) Y. Leng, G. Yang, Y. Hu and L. Zheng: J. Mater. Sci. **35** (2000) 2061.
10) Y. Isono and T. Tanaka: JSME Int. J. Ser. A: Mech. Mater. Eng. **42** (1999) 158.
11) T. Y. Tsui and G. M. Pharr: J. Mater. Res. **14** (1999) 292.
12) J. M. Haile: *Molecular Dynamics Simulation: Elementary Methods* (New York, Wiley, 1992).
13) Y. Isono and T. Tanaka: JSME Int. J. Ser. A: Mech. Mater. Eng. **40** (1997) 211.
14) K. Maekawa and A. Itoh: Wear **188** (1995) 115.
15) T. H. Fang and C. I. Weng: Nanotechnology **11** (2000) 148.
16) K. L. Johnson: *Contact Mechanics* (Cambridge University Press, Cambridge, 1985).